J Mater Sci (2011) 46:1542–1550
DOI 10.1007/s10853-010-4959-5

Crystallization behavior of poly (vinylidene fluoride)/multi-walled carbon nanotubes nanocomposites

Kai Ke · Rui Wen · Yu Wang · Wei Yang · Bang-Hu Xie · Ming-Bo Yang

Received: 27 July 2010 / Accepted: 28 September 2010 / Published online: 14 October 2010

Abstract The non-isothermal and isothermal crystallization of poly (vinylidene fluoride) (PVDF)/multiple-walled carbon nanotubes (MWNTs) composites containing pristine (MWNT1) and carboxyl group (–COOH) functionalized MWNT (MWNT2) were investigated. The effects of MWNT on the crystallization behavior of PVDF were dependent on the dispersion state of MWNT. Pristine MWNT could increase the nucleation due to better dispersion, and thus, PVDF/MWNT1 composites exhibited higher crystallization peak temperatures (T_{cp}s) and crystallinities (X_cs) compared with PVDF/MWNT2 composites. Meanwhile, the formation of MWNT network confined the growth of crystals. For the isothermal crystallization, MWNT acted as nucleating agents, and the crystallization rate constant k was increased with the addition of MWNT. Besides, the half crystallization time, $t_{0.5}$, was remarkably shortened with the increase of MWNT content, especially for the pristine MWNT.

Introduction

Poly vinylidene fluoride (PVDF) is a semi-crystalline thermoplastic polymer which is used widely in various applications such as chemical industry, semiconductor, medical and defense industries, constructions as well as in lithium-ion batteries. PVDF is also notable for its polymorphism, such as the *tt* (all-trans), tg^+tg^-(trans gauche$^+$ trans gauche$^-$), and ttg^+ttg^- conformation, which are referred to as α, β, and γ phase, respectively [1]. Usually, α-phase is the dominant crystalline phase in PVDF. However, β-phase PVDF exhibits piezo-, pyro-, and ferroelectric activities, which lead to the applications of sensors and transducers [2]. Therefore, the preparation of β-phase PVDF has attracted much interest, and many processing methods have been put forward. [3–9] In addition, PVDF possesses excellent properties such as favorable mechanical properties, which are related to the α-phase or other phases. The relatively low cost, good processability, and excellent mechanical properties of PVDF, compared with other fluoropolymers, make it widely used in chemical and electronic industry. So, it is interesting and vital to study the crystallization behaviors of PVDF composites for a thorough understanding of their mechanical and thermal properties.

Carbon nanotubes (CNTs) possess remarkable mechanical and physical properties, such as high stiffness, strength, and conductivity. Therefore, it has been widely used as a reinforcing nano-filler in polymer composites [10–12]. At the same time, the related crystallization behavior of the CNT-filled semi-crystalline polymers such as isotactic polypropylene (iPP) [13], PE [14], PLLA [15], PTT [16] etc. were widely studied. The crystallization behavior of CNT-filled PVDF nanocomposites has also been extensively reported. For example, Poly (methyl methacrylate) (PMMA)-grafted MWNTs were used to prepare PVDF/MWNT composite [17], and the nucleation effect was found to be suppressed when PMMA was grafted onto the nanotubes. Kim et al. [18] found that MWNT not only could act as a nucleating agent to produce polar β-form crystals of PVDF but also reduced the

K. Ke · R. Wen · Y. Wang · W. Yang (✉) · B.-H. Xie · M.-B. Yang
College of Polymer Science and Engineering, Sichuan University, State Key Laboratory of Polymer Materials Engineering, Chengdu 610065, Sichuan, China
e-mail: ysjsanjin@163.com

supercooling required for PVDF crystallization and the size of spherulites. Huang et al. [19] found that MWNT with high aspect ratio had more zigzag carbon atoms on the surface, which matched with the all-trans conformation of β-phase PVDF and facilitated the crystallization of β-phase PVDF. Levi et al. [20] found that the thin films of solution-cast PVDF/CNTs composites exhibited enhancements in both the pyroelectric response and mechanical transduction over pure PVDF, which indicated the nanotubes enhanced the formation of piezoelectric β-phase PVDF. He et al. [21] found that the PVDF crystalline phases could be greatly altered from α- to β-form by the incorporation of MWNTs when dimethyl sulfoxide (DMSO) was used as the solvent to prepare the composite.

As can be seen, most studies related with the crystallization of PVDF/MWNT composites focused on the phase transition of α-phase to β-phase or the formation of β-phase PVDF crystals, because the plane zigzag conformation of MWNT can facilitate the formation of β-phase PVDF crystals [22–24]. However, MWNT with different surface chemistry will affect the crystallization behavior of PVDF/MWNT composite inevitably. In this article, PVDF and two kinds of MWNT with different surface characteristics were melt blended, and the non-isothermal and isothermal crystallization behavior of the composites were investigated.

Experiment section

Materials

The PVDF powder, FR 901, with a weight average molecule weight of $M_w = 28.5 \times 10^4$ g/mol and a polydispersity index of 1.93, was purchased from 3F Co. Ltd., Shanghai, China. Two different kinds of MWNTs with different aspect ratios and functional treatments were adopted. The first kind of MWNT, denoted as MWNT1, was untreated, having a diameter of 10–20 nm and a length of $\sim$30 μm; the other kind of MWNT, denoted as MWNT2, contains 3.85 wt% carboxyl groups on the surface, having a diameter of less than 8 nm and a length of $\sim$30 μm. Both kinds of MWNT were purchased from Chengdu Organic Chemistry Co. Ltd., Chinese Academy of Science.

Preparation of PVDF/MWNT composites

Compared with the solution mixing method, melt compounding is much more convenient, economic, and environment-friendly. Consequently, the PVDF/MWNT composites were prepared by melt compounding in a torque rheometer at 220 °C. First, a certain amount of PVDF powder was added into the chamber of torque rheometer and plasticized, then, the MWNT with preset proportion was incorporated into the melt, and finally, the rest of PVDF powder according to the formulations was added and plasticized for 5 min. The loading of the two kinds of MWNT in the composites ranged from 0 to 5.0 wt%. The resultant samples were named according to their compositions, and the detailed information of the samples was listed in Table 1.

Table 1 The detailed information of PVDF/MWNT composites

Samples	Type of MWNT	Content of MWNT
PVDF/0.5% MWNT1	Un-functionalized	0.5 wt%
PVDF/2% MWNT1	Un-functionalized	2.0 wt%
PVDF/5% MWNT1	Un-functionalized	5.0 wt%
PVDF/0.5% MWNT2	–COOH	0.5 wt%
PVDF/2% MWNT2	–COOH	2.0 wt%
PVDF/5% MWNT2	–COOH	5.0 wt%

Tests and characterizations

DSC

The crystallization behaviors of the samples were studied by means of a differential scanning calorimeter Q20 (TA, USA). For the non-isothermal crystallization behaviors, the samples were first heated up to 200 °C at a rate of 10 °C/min under a nitrogen atmosphere and held at 200 °C for 5 min to eliminate the influence of thermal history. After that, the samples were cooled to 40 °C at a rate of 10 °C/min, and then heated again to 200 °C at a heating rate of 10 °C/min, with samples of about 3–5 mg; the crystallization and melting curves were recorded. For the isothermal crystallization behaviors, the samples were heated under the same condition as for non-isothermal crystallization test but cooled to 148 °C at a rate of 200 °C/min to perform isothermally crystallization for 15 min, and then heated up again to 200 °C at 10 °C/min and held at 200 °C for 5 min to carry out another isothermally crystallization. In this way, seven temperatures for isothermal crystallization, 148, 146, 144, 142, 140, 138, and 136 °C, were used.

SEM

The dispersion of MWNT in PVDF was characterized with a JEOL JSM-5900LV scanning electron microscope (SEM) at an accelerating voltage of 20 kV. The samples were left in liquid nitrogen for 40 min and then impact fractured for SEM analysis. The freshly fractured surface was gold sputtered before SEM observation.

Dynamical rheology tests

The viscoelastic properties of PVDF/MWNT composites were studied by stress controlled dynamic rheometer AR2000ex (TA, USA), in a parallel plate geometry. The composites were compression-molded into disks with the diameter of 25 mm and the thickness of 1 mm at 220 °C and 10 MPa. The dynamic rheological tests of these samples were conducted at 200 °C. The strain and oscillation frequency range were 1.0% and 0.01–70 Hz, respectively.

Results and discussion

Dispersion of MWNT in PVDF

Figure 1 shows the morphology of the melting compounded PVDF/MWNT composites. It is clear that more aggregates of MWNT2 (with carboxyl groups) can be seen in some regions as marked by cycles. On the contrary, the untreated MWNT1 dispersed relatively more uniformly. As we know, MWNTs are inclined to aggregate due to the van der Waals interactions between the nanotubes [25]. Consequently, the strong shear effects, such as intense mechanical stirring and high rotation speed of the screw in extruders, are often used to improve the dispersion of CNTs [26]. The introduction of carboxyl groups onto MWNT surface will increase the surface polarity of MWNT, and the adsorption between PVDF chains (low polarity) and the MWNT will be reduced. So, the pristine MWNT shows higher degree of adsorption with PVDF chains, resulting in a relatively better dispersion state in the PVDF matrix.

It has been proved that the dynamic rheological behavior can also be used to estimate the dispersion of nanotubes in CNTs polymer composites [26, 27]. The storage modulus (G') and loss tangent angle (tan δ) will become more and more independent on the frequency at low frequency range with the increasing content or the improved dispersion of CNTs. The frequency dependence of the G' and tan δ for PVDF/MWNT composites is shown in Figs. 2 and 3, respectively. It can be seen that the storage modulus increased with increasing content of MWNT for both composites. Obviously, with the incorporation of 2 and

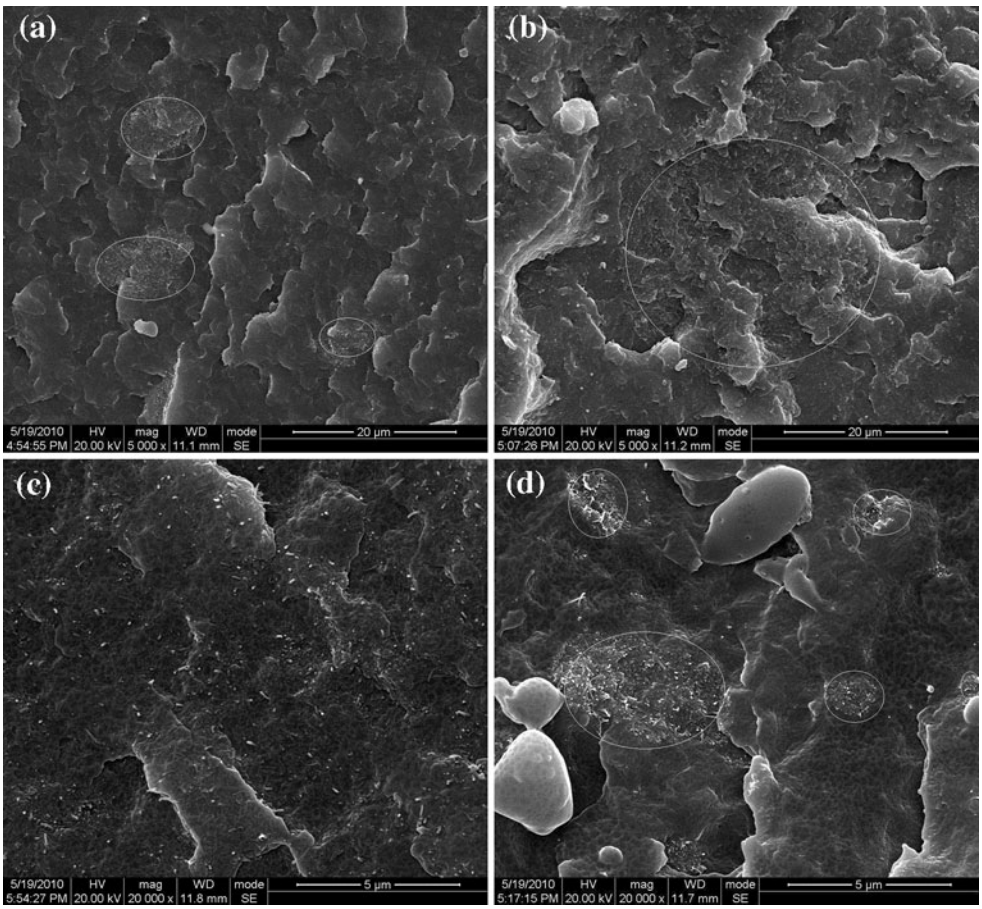

Fig. 1 SEM images of PVDF/MWNT composites. **a** PVDF/0.5%MWNT1, **b** PVDF/0.5%MWNT2, **c** PVDF/5%MWNT1, and **d** PVDF/5%MWNT2

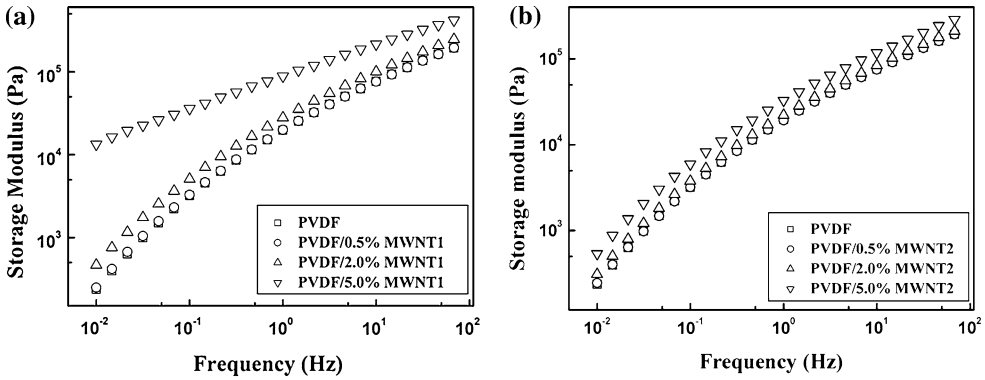

Fig. 2 Dynamic storage modulus versus frequency for PVDF/MWNT1 (**a**) and PVDF/MWNT2 (**b**) composites

5 wt% content of MWNT, PVDF/MWNT1 composites exhibited a higher G' than that of PVDF/MWNT2 composites, especially at low frequencies. This shows that MWNT1 has a better dispersion in the PVDF matrix compared with MWNT2, which agrees with the result of SEM observations. As shown in Fig. 3, similar difference in tan δ for the composites counterparts can be observed. Lower values of tan δ reflect more effective restriction effect of the nanotubes on the relaxation of PVDF chains, and this restriction effect is directly dependent on the dispersion of MWNTs. In all, the higher G' and lower tan δ at low frequency range for all counterparts indicate a better dispersion state of MWNT1 than that of MWNT2 in the PVDF matrix.

Non-isothermal crystallization

Figures 4 and 5 show the non-isothermal crystallization and the following melting behaviors of PVDF/MWNT composites, and the detailed data are listed in Table 2. In Figs. 4 and 5, the peak temperature (T_{cp}) of non-isothermal crystallization process shifts to higher temperatures visibly for the composites, compared with that of neat PVDF. It can be seen from Table 2 that the maximum T_{cp} is about 9 °C higher than that of pure PVDF. In addition, T_{cp}s of the PVDF/MWNT1 composites are higher than the counterparts of PVDF/MWNT2, which suggests that the better dispersion of MWNT1 resulted in a greater increase of the nucleation compared with MWNT2. While for the

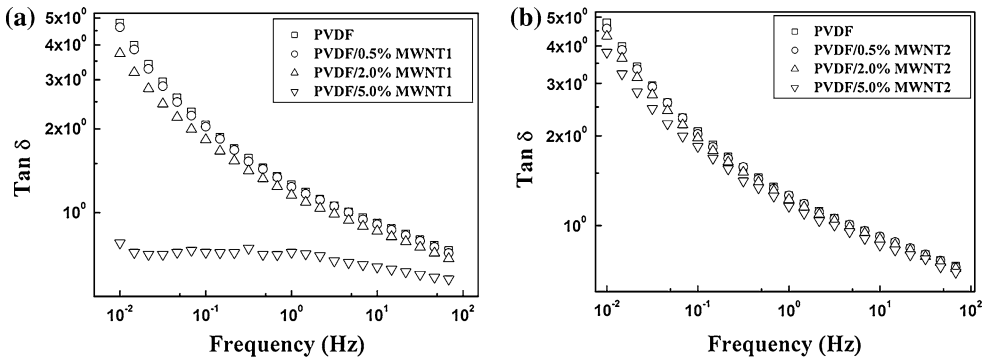

Fig. 3 Tan δ versus frequency for PVDF/MWNT1 (**a**) and PVDF/MWNT2 (**b**) composites

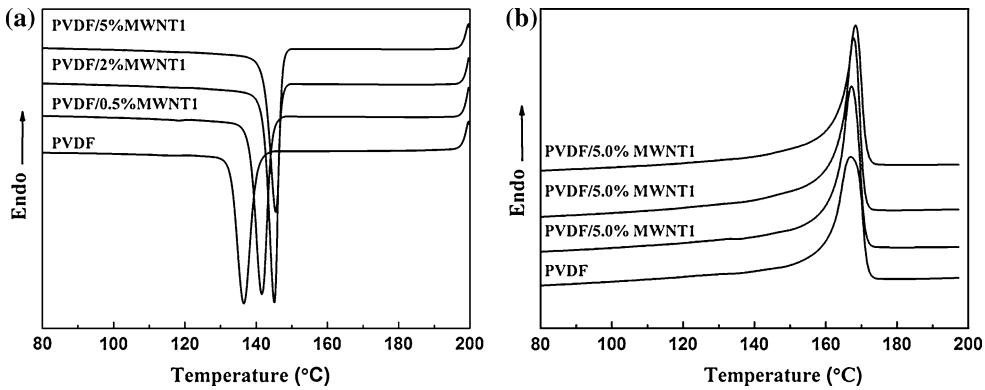

Fig. 4 DSC non-isothermal crystallization curves (**a**) and the following melting curves (**b**) for PVDF/MWNT1 composites

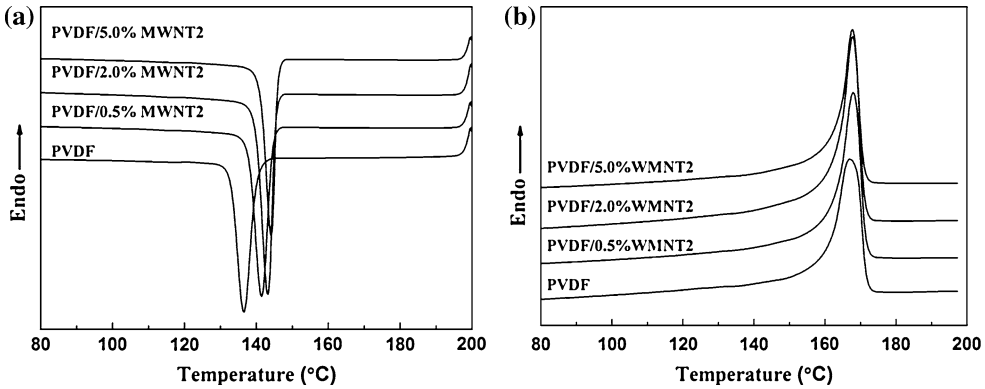

Fig. 5 DSC non-isothermal crystallization curves (**a**) and the following melting curves (**b**) for PVDF/MWNT2 composites

Table 2 DSC parameters of non-isothermal crystallization and the following melting process for PVDF/MWNT composites

Samples	T_{cp} (°C)	ΔH_c (J/g)	T_{mp} (°C)	ΔH_{mp} (J/g)	X_c (%)
Pure PVDF	136.52	43.25	167.03	35.52	33.96
PVDF/0.5%MWNT1	141.59	49.34	167.28	40.39	38.81
PVDF/2.0%MWNT1	145.11	48.64	167.83	44.28	43.20
PVDF/5.0%MWNT1	145.49	43.95	168.36	36.85	37.08
PVDF/0.5%MWNT2	141.44	46.88	167.94	38.86	37.34
PVDF/2.0%MWNT2	143.15	48.17	167.77	39.91	38.93
PVDF/5.0%MWNT2	144.09	44.08	167.70	36.42	36.65

T_{cp} crystallization peak temperature, ΔH_c heat release of crystallization, T_{mp} melting peak temperature, ΔH_m heat of fusion, and X_c mass fraction crystallinity

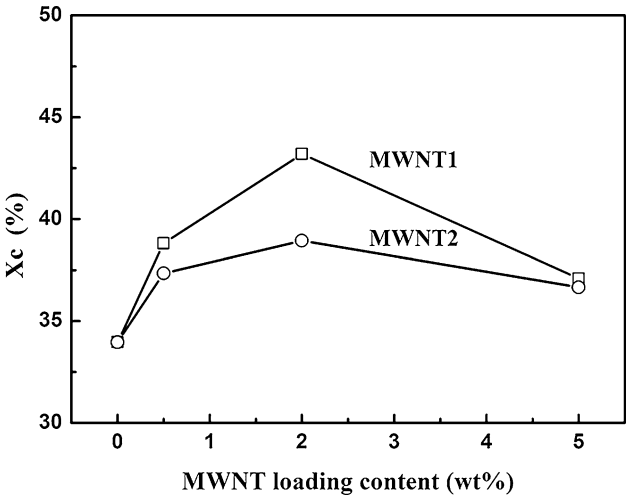

Fig. 6 The dependence of crystallinity on MWNT loading for PVDF/MWNT composites

crystallization heat enthalpy (ΔH_c) and heating enthalpy of fusion (ΔH_m), PVDF/MWNT composites with lower MWNT content are higher. This may be due to that the higher loading of nanotubes will have a greater restriction effect on the mobility of PVDF chains and decrease the crystal growth rate. As for the melting peak temperature, T_{mp}, PVDF/MWNT1 composites have a higher value than those of PVDF/MWNT2 composites except for the sample containing 0.5% MWNTs. This observation is probably caused by the fact that the interaction between the PVDF matrix and MWNT2 is stronger than that for MWNT1 because a stronger constraint effect will go against the thickening of the crystals and results in a lower T_{mp}. Besides, the smaller molecular weight chains are adsorbed to nanotubes [28], which may result in stronger restriction of PVDF chains mobility during the melting process. The probable reason is that shorter chains are preferentially adsorbed onto the interface because of their relatively quick diffusion by kinetic factors [29].

The degree of mass crystallinity (X_c) of the PVDF/MWNT composites was calculated using the following equation: [30]

$$X_c = (\Delta H_m)/\psi\ (\Delta H_m^0) \times 100\% \quad (1)$$

where ΔH_m is the heating enthalpy of fusion from the recorded heating scan, ψ is the PVDF content in the PVDF/MWNT composites, and ΔH_m^0 is the heat of fusion of 100% crystalline PVDF. Here, the value of 104.6 J/g is used for ΔH_m^0 [31]. The calculated results are also listed in Table 2. It can be seen easily that the crystallinity of the composite is significantly increased with the incorporation of MWNT, and the maximal increment of X_c compared with that of neat PVDF is about 9.2%. Besides, the increases of X_c for PVDF/MWNT1 composites are greater than those for PVDF/MWNT2 composites, which can be more directly seen in Fig. 6. Besides, in Fig. 6, it also can be observed that X_c first increases with the incorporation of the two kinds of MWNTs and both reaches the maximum at 2 wt% loading, then decreases with further increasing of MWNT content. The probable interpretation is that the MWNT can affect the crystallization behavior of PVDF composites with different roles in the nucleation stages and crystal growth process. For one thing, the increase of MWNT loading can increase the nucleation; for another, high

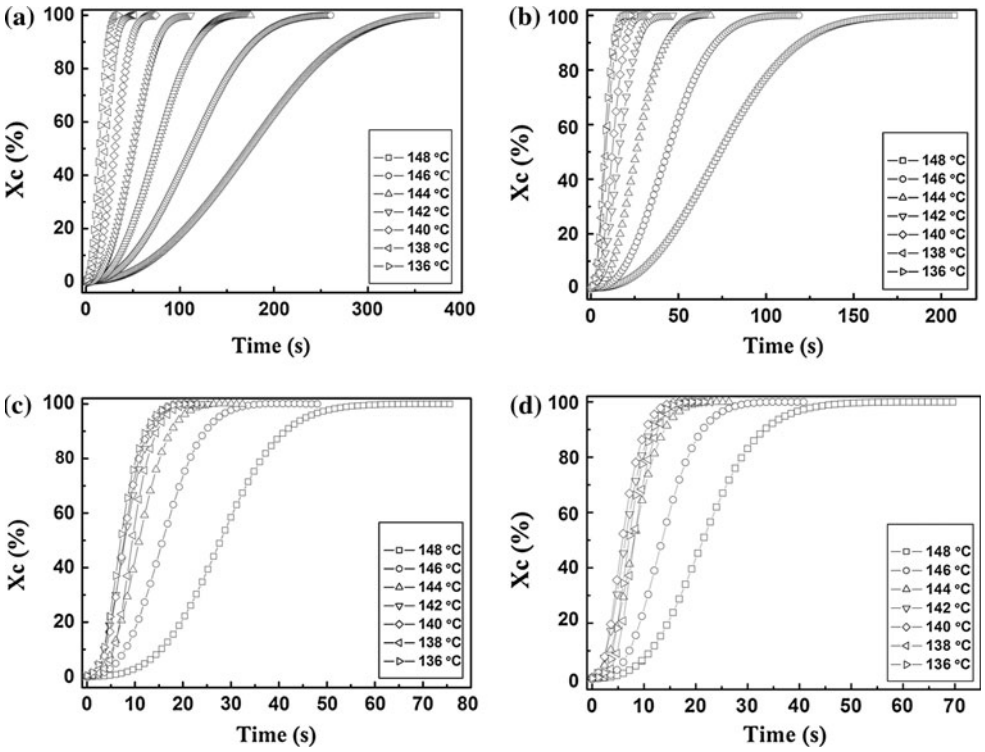

Fig. 7 Relative crystallinity versus time during isothermal crystallization at different temperatures for **a** neat PVDF, **b** PVDF/0.5%MWNT1, **c** PVDF/2%MWNT1, and **d** PVDF/5%MWNT1

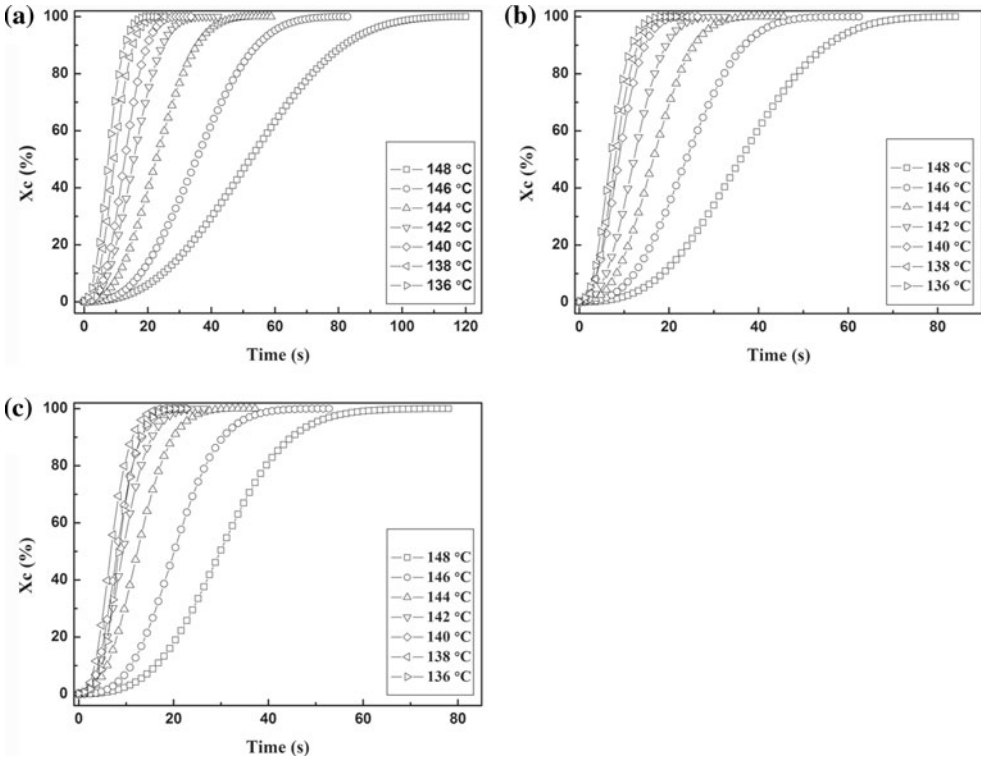

Fig. 8 Relative crystallinity versus time during isothermal crystallization at different temperatures for **a** PVDF/0.5%MWNT2, **b** PVDF/2%MWNT2, and **c** PVDF/5%MWNT2 composites

content of MWNT will reduce growth rate of crystals by hindering the motion of PVDF chains due to the interaction of nanotube–nanotube and nanotube–polymer [32, 33]. Similar phenomenon was observed on the crystallization kinetics of nylon 66/MWNT modified by poly (hexamethylene adipamide) composite [30].

Isothermal crystallization

Isothermal crystallization behaviors of PVDF/MWNT composites were examined at several temperatures, and Figs 7 and 8 show the variation of relative crystallinity $X(t)$ with crystallization time t of PVDF/MWNT composites. In general, the relative degree of crystallinity at time t, $X(t)$, is defined as: [34]

$$X_t = \frac{X_c(t)}{X_c(t_\infty)} = \frac{\int_0^t \frac{dH(t)}{dt}\,dt}{\int_0^{t_\infty} \frac{dH(t)}{dt}\,dt} = \frac{\Delta H_t}{\Delta H_\infty} \quad (2)$$

where dH/dt is the rate of heat evolution, $\Delta H_t$is the heat generated at time t, and $\Delta H_\infty$is the total heat. From Figs. 7 and 8, it can be seen that the characteristic sigmoid isotherms shift to a shorter time with decreasing isothermal crystallization temperature (T_c), while the crystallization rate becomes faster. So, the crystallization is accelerated by the incorporation of MWNT. In order to understand how the MWNT affect the crystallization behavior of PVDF/MWNT composites, the crystallization kinetics of the composites is analyzed, and here the classical Avrami equation [35] as follows is adopted.

$$1 - X_c = \exp(-kt^n) \quad (3)$$

where X_c is the relative crystallinity at time t, k is a temperature-dependent constant, and n is an exponent which contains the contributions related to the crystal growth geometry and the time dependency of the nucleation rate. The Avrami parameter n and crystallization rate constant k can be determined by taking the double logarithmic chart by $\ln[-\ln(1 - X_c)]$ versus $\ln t$ according to Eq. 3.

The data of kinetics parameters for different T_cs and contents of MWNT for PVDF/MWNT1 and PVDF/MWNT2 composites are calculated and summarized in Tables 3 and 4, respectively. As shown in Table 3, the Avrami parameter n is larger than 2, indicating a heterogeneous nucleation process. The incorporation of MWNT leads to an increase in the value of n to some extent as well. Similar results can be observed in PVDF/MWNT2 composites, as shown in Table 4. In addition, both in Tables 3 and 4, with the incorporation of MWNT, the Avrami exponent n increases visibly at relative high isothermal crystallization temperatures. It is probable that MWNT acts as a good heterogeneous nucleation agent, which enhances the nucleation and accelerates the crystallization process [16].

Note that the value of k also rises evidently with the increasing of MWNT content, indicating the incorporation of MWNT accelerates the crystallization kinetics of the composites. Moreover, it seems that PVDF/MWNT1 composites have a higher k than that of PVDF/MWNT2 composites except for the samples containing 0.5% MWNT, which reveals that PVDF/MWNT1 composites have a faster crystallization process than that of PVDF/MWNT2 composites. The half crystallization time, $t_{0.5}$, can be used to estimate the influence of MWNT on the isothermal crystallization behavior as well. From Tables 3 and 4, it can be seen that $t_{0.5}$ reduces sharply with the decrease of T_c and increasing of MWNT loading. Therefore, the incorporation of MWNT has a drastic influence on the crystallization of the composites. In addition, it is easy to find that $t_{0.5}$ exhibits a slight increase with the rise of T_c for samples with high loading levels of MWNTs, which indicates that the crystallization behavior is confined to some extent owing to the restriction of the mobility of the molecular chains [36]. Figure 9 shows the influence of T_c and MWNT content on $t_{0.5}$. It is clear that the two kinds of MWNTs have different effects on the half crystallization time. PVDF/0.5%MWNT2 composite has a shorter $t_{0.5}$

Table 3 Kinetic parameters for neat PVDF and PVDF/MWNT1 nanocomposites during isothermal crystallization

Sample name	T_c (°C)	n	k	$t_{0.5}$ (s)
Pure PVDF	148	2.0622	1.51E−5	174.17
	146	2.24759	1.74E−5	113.49
	144	2.40759	2.17E−5	74.55
	142	2.64677	2.21E−5	49.31
	140	2.44124	1.64E−4	30.92
	138	2.38472	5.18E−4	19.89
	136	2.20884	2.10E−3	13.21
PVDF/0.5%MWNT1	148	2.46758	1.71E−5	74.04
	146	2.57392	4.03E−5	43.74
	144	2.55057	1.66E−4	25.88
	142	2.30724	1.10E−3	16.06
	140	2.60362	9.97E−4	11.77
	138	2.31608	4.77E−3	8.85
	136	2.37181	5.31E−3	7.49
PVDF/2.0%MWNT1	148	2.9324	3.82E−5	27.82
	146	2.59943	5.29E−4	15.78
	144	2.52551	1.65E−3	10.98
	142	2.31105	5.70E−3	9.24
	140	2.73065	2.49E−3	3.71
	138	3.03392	6.96E−4	4.35
	136	2.5571	4.63E−3	3.47
PVDF/5.0%MWNT1	148	2.81558	1.21E−4	21.06
	146	2.94832	3.14E−4	13.27
	144	2.2112	6.74E−3	7.82
	142	2.14666	1.24E−2	6.32
	140	2.21448	1.31E−2	5.75
	138	2.73134	2.26E−3	7.96
	136	2.40774	6.13E−3	6.99

T_c the temperature of isothermal crystallization, n Avrami parameter, k the crystallization rate constant, and $t_{0.5}$ half crystallization time

Table 4 Kinetic parameters for PVDF/MWNT2 nanocomposites during isothermal crystallization

Sample name	T_c (°C)	n	k	$t_{0.5}$ (s)
PVDF/0.5%MWNT2	148	2.21838	8.14E−5	52.25
	146	2.57698	6.17E−5	35.63
	144	2.5573	2.32E−4	22.60
	142	2.46171	8.01E−4	15.64
	140	2.76863	5.85E−4	12.96
	138	2.41405	2.89E−3	9.82
	136	2.31422	6.39E−3	7.44
PVDF/2.0%MWNT2	148	2.61805	5.40E−5	35.95
	146	2.65764	1.49E−4	23.91
	144	2.64124	4.20E−4	16.27
	142	2.4718	1.45E−3	11.91
	140	2.22096	5.72E−3	8.60
	138	2.49384	3.81E−3	7.90
	136	2.27344	8.51E−3	7.75
PVDF/5.0%MWNT2	148	2.60652	7.98E−5	30.03
	146	2.85982	1.19E−4	20.10
	144	2.43977	1.46E−3	12.20
	142	2.33374	3.76E−3	9.42
	140	2.64142	2.53E−3	7.91
	138	2.5311	5.09E−3	6.76
	136	2.6541	2.21E−3	8.42

T_c the temperature of isothermal crystallization, n Avrami parameter, k the crystallization rate constant, and $t_{0.5}$ half crystallization time

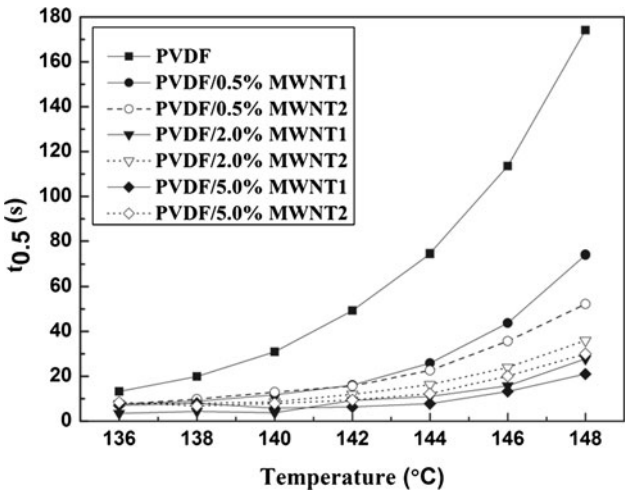

Fig. 9 Half crystallization time as a function of isothermal crystallization temperature for PVDF and PVDF/MWNT composites

than that of PVDF/0.5%MWNT1 composite at low T_cs, but the $t_{0.5}$s of other PVDF/MWNT2 composites are visibly higher than their counterparts of PVDF/MWNT1 composites. The lower $t_{0.5}$ of PVDF/MWNT1 composites reveals that the MWNT1 has a more visible acceleration effect on the isothermal crystallization process of PVDF/MWNT composites than that of MWNT2, due to the better dispersion state of MWNT with the adsorption of MWNT and PVDF.

Conclusion

The non-isothermal and isothermal crystallization behaviors of PVDF/MWNT composites were studied. The influence of MWNT on the crystallization of PVDF is dependent on the dispersion and surface chemistry of MWNT. The nucleation effect of MWNT1 is more obvious than that of MWNT2 because of a relatively better dispersion of MWNT1 in PVDF matrix as proved by the results of SEM and dynamic rheology tests. The surface chemical properties can affect the crystallization of PVDF in two aspects: one is its effect on the dispersion of MWNT and the other is the constraint effect of the interactions between PVDF and MWNT on the growth of crystals.

Acknowledgements The authors gratefully acknowledge the financial support of National Natural Science Foundation of China (Grant No. 20734005 and 50973074) and the Program for New Century Excellent Talents in University (NCET-08-0382). We are also heavily indebted to Mr. Zhu Li from Center of Analysis and Test of Sichuan University for careful SEM observation.

References

1. Lovinger AJ (1983) Science 220:1115
2. Broadhurst MG, Davis GT (1981) Ferroelectrics 32:177
3. Narula GK, Pillai PKC (1989) J Mater Sci Lett 8:627
4. Gregorio JR, Ueno EM (1999) J Mater Sci 34:4489. doi: 10.1023/A:1004641322544
5. Hsu SL, Lu FJ, Waldman DA, Muthukumar M (1985) Macromolecules 18:2583
6. Sencadas V, Gregorio R Jr, Lanceros-Mendez S (2009) J Macromol Sci Part B Phys 48:514
7. Gregorio R, Cestari M (1994) J Polym Sci Part B Polym Phys 32:859
8. Dillon DR, Tenneti KK, Li CY, Ko FK, Sics I, Hsiao BS (2006) Polymer 47:1678
9. He QJ, Zhang AM (2008) J Mater Sci 43:820. doi: 10.1007/s10853-007-2153-1
10. Allaoui A, Bai S, Cheng HM, Bai JB (2002) Compos Sci Technol 62:1993
11. Zou YB, Feng YC, Wang L, Liu XB (2004) Carbon 42:271
12. Zhang FH, Wang RG, He XD, Wang C, Ren LN (2009) J Mater Sci 44:3574. doi:10.1007/s10853-009-3484-x
13. Xu DH, Wang ZG (2008) Polymer 49:330
14. Haggenmueller R, Fischer JE, Winey KI (2006) Macromolecules 39:2964
15. Zhao YY, Qiu ZB, Yang WT (2008) J Phys Chem B 112:16461
16. Xu Y, Jia HB, Piao JN, Ye SR, Huang J (2008) J Mater Sci 43:417. doi:10.1007/s10853-007-2161-1
17. Wang M, Shi JH, Pramoda KP, Goh SH (2007) Nanotechnology 18:235701
18. Kim GH, Hong SM (2007) Mol Cryst Liq Cryst 472:161/[551]

19. Huang XY, Jiang PK, Choung K, Liu F, Yin Y (2009) Eur Polym J 45:377
20. Levi N, Czerw R, Xing SY, Iyer P, Carroll DL (2004) Nano Lett 4:1267
21. He LH, Sun J, Zheng XL, Xu Q, Song R (2010) J Appl Polym Sci. doi:10.1002/app.32907
22. Nam YW, Kim WN, Cho YH et al (2007) Macromol Symp 249–250:478
23. Mago G, Kalyon DM, Fisher FT (2008) J Nanomater 2008: (Article ID 759825, 8 pages)
24. Zhao ZD, Zheng WT, Yu WX, Long BH (2009) Carbon 47:2118
25. Pötschke P, Dudkin SM, Alig I (2003) Polymer 44:5023
26. Huang YY, Terentjev EM (2008) Int J Mater Form 1:63
27. Zhang QH, Fang F, Zhao X, Li YZ, Zhu MF, Chen DJ (2008) J Phys Chem B 112:12606
28. Grossiord N, Miltner HE, Loos J, Meuldijk J, Mele BV, Koning CE (2007) Chem Mater 19:3787
29. Jiang J, Liu H, Hu Y (1998) Macromol Theory Simul 7:113
30. Li LY, Li CY, Ni CY, Rong L, Hsiao B (2007) Polymer 48:3452
31. Marega C, Marigo A (2003) Eur Polym J 39:1713
32. Jog JP (2006) Mater Sci Technol 22:797
33. Papageorgious GZ, Achilias DN, Karayannidis GP (2005) Therm Acta 427:117
34. Cebe P, Hong SD (1986) Polymer 27:1183
35. Avami M (1941) J Chem Phys 9:177
36. Hu X, Lesser AJ (2003) J Polym Sci Part B Polym Phys 41:2275